ELSEVIER

Ceramics International 27 (2001) 57–62

CERAMICS
INTERNATIONAL

www.elsevier.com/locate/ceramint

Population balance model for solid state sintering
I. Pore shrinkage and densification

Manjunath Subbanna [a], P.C. Kapur [a], Pradip [a,*], S.G. Malghan [b]

[a] *Tata Research Development and Design Centre, Plot # 54 B, Hadapsar Industrial Estate, Pune 411 013, India*
[b] *National Institute of Standards and Technology, 100 Bureau Drive, Gaithersburg, MD 20899-0001, USA*

Received 14 January 2000; received in revised form 8 February 2000; accepted 2 March 2000

Abstract

A general population balance model incorporating the rate of shrinkage of individual pores during solid state sintering of ceramics is described. The kinetics of pore shrinkage is assumed to follow a simple power law with floating value of the exponent. The resulting equation of continuity is solved for the evolution of pore size distribution in time by a transformation technique. The simulated pore size distributions for a number of ceramic oxide systems are in good agreement with experimental data generated in-house as well as from published sources. The model can be embedded in a coupled phenomenon of densification and grain growth, as shown in Part II. © 2001 Elsevier Science Ltd and Techna S.r.l. All rights reserved.

Keywords: A. Sintering; B. Porosity

---

1. Introduction

Solid state sintering involves two major phenomena occurring simultaneously, that is, pore shrinkage accompanied with grain growth. The evolution of microstructure during sintering that is the kinetics of change in the size distribution of grains and pores is of great interest to the materials processing industry. While a number of advances have taken place in our understanding of the physics of sintering [1–4], very little has been accomplished in optimizing the industrial processes involving size distributed powder compacts. In our view what is lacking is a mathematical framework which lends itself to rigorous engineering optimization on an industrial scale. Optimization of sintering cycles for example, which is currently being done by trial and error, is essentially aimed at achieving zero porosity (fully dense compact) with minimum grain growth.

The objective of our efforts has therefore been to utilize a population balance paradigm to quantitatively and elegantly describe the sintering process incorporating the kinetics of pore shrinkage and grain growth. The model thus developed as illustrated in this paper (parts I and II) can be utilized to simulate and optimize the sintering process for a given objective function.

1.1. Intermediate stage of sintering

A green ceramic compact consists of a complex network of inter-connected pores that are bounded by the surface of the particles. In course of sintering, concurrently with grain growth, the pore structure undergoes massive changes with an overall reduction in porosity. The evolution of the pore structure is thus not only closely related to the densification kinetics [5], it also exerts a decisive influence on the development of the microstructure [6] and a host of mechanical, electrical and optical properties that depend on it [7–9].

Based on the geometry of pores and their distribution in the ceramic matrix, the phenomenon of solid state sintering is traditionally divided into a number of sequential stages [10]. The initial stage is one where particles maintain their individual identity while neck growth takes place between them with relatively limited shrinkage of the compact. The intermediate stage, where the particles lose their individual identity, porosity is modelled as a network of interconnected channels running along the grain edges, and most of the densification and a great deal of grain growth occurs. And the final stage, where pores are pinched off and lie isolated either at

---

* Corresponding author. Fax: +91-20-681-0921.
E-mail address: pradip@pune.tcs.co.in (Pradip).

PII: S0272-8842(00)00043-2

grain corners or enclosed within grains, and normal grain growth followed possibly by abnormal growth takes place. Even though there may not always be distinct demarcations between these stages, a quantitative description of the sintering process is greatly facilitated by modelling the various stages separately. The transitory regime that prevails in the intermediate stage of sintering, is deemed technologically the most important stage.

In order to utilize the recent advances made in our understanding of sintering processes, there is a need to develop a generalized, quantitative framework capable of describing sintering in real powder systems. It is widely recognised that the laboratory investigations carried out under controlled environments, on ideal geometries and with monosize particles, though extremely useful in understanding the physics of sintering, are usually too simplified to be able to capture and describe the complexity of industrial scale sintering. The complexity of industrial scale operations stems from the following important sources — one, the powder compacts always possess a distribution of crystallites and pores; second, the sintering/densification process is not at steady state; third, more than one mechanism of diffusion may be applicable. It is for this reason, that the steady state solutions (e.g. LSW theory [11,12]) based on a particular mechanism of sintering may not describe the process well.

Our attempt has been to utilize a population balance paradigm for describing solid state sintering in ceramic systems. It is capable of describing the complex process of sintering in a reasonably elegant way; in particular the above mentioned complexities are taken care of in our formulation to some extent, at least. The model, once validated with experimental data for a given system can then be utilized for a variety of applications including detailed simulation trials aimed towards optimization and control. The utility of such a mathematical model, which incorporates the essentials of a process in sufficient detail, in optimizing industrial processes need not be overemphasised. There is no currently available methodology to optimize the sintering schedule (time–temperature cycle) for a given sintering system. The successful implementation of our approach for a set of solid state sintering process systems is presented in this paper consisting of two parts — the first on densification and the second on grain growth.

The kinetics of grain growth during the intermediate stage of sintering depends on the rate of shrinkage of pores. As such, a comprehensive and detailed population balance based model of sintering should address grain growth and pore shrinkage simultaneously, as proposed by Pradip [13]. In this framework, the coupled partial differential equations of grain growth and pore shrinkage must be solved together in order to track the evolution of the microstructure. This, however, is not a trivial task due to modelling and computational difficulties as well as lack of prior knowledge of the values of many constants and parameters present in the model equations. In general, the process of grain growth cannot be analyzed realistically independent of the pore shrinkage [14–18]. However, many examples exist in the literature, which suggest that the pore shrinkage may be examined in isolation from the grain growth [19–23]. This is because pore shrinkage, which occurs primarily by material transport into the pores, may be treated as a process of vacancy diffusion into grain boundaries [20, 24]. Therefore, it is possible to conceive of a tractable two-part strategy for analyzing the sintering process. First, pore shrinkage is modelled in isolation at an appropriate level of sophistication and, second, the resulting model is embedded in a coupled grain growth and densification model. In the first part of the paper, we focus on the development of a semi-empirical, but fairly general, model of the kinetics of pore shrinkage and the evolution of pore size distribution in course of sintering.

2. The model

In general, the starting point for analysis and modelling of pore shrinkage (and or grain growth) is the identification and incorporation of an appropriate material transport mechanism(s) into a plausible model of the process kinetics. At a somewhat simpler level, however, it is possible to construct a model without an explicit reference to the material transport mechanism. It is assumed that the operating mechanism is embedded into the constants and parameters of the rate equation. An example of this approach is the model of Hogg and Hwang [21] in which the pores, considered cylindrical in shape, undergo only radial shrinkage. In other words, the total pore length is conserved at all times. The rate of shrinkage of the pore is assumed to vary inversely as the square of the pore radius. The model was applied to a typical set of data pertaining to sintering of alumina. Tomandl [22] presented a quantitative model of densification taking into account the size distribution of grains and pores. The pores were perceived as spherical and the rate of change was assumed proportional to the inverse of the square of the radius. Again, the model was applied to the sintering data for alumina compacts.

The power law in the aforementioned models is highly specialized in view of the assumption that the shrinkage rate is inversely proportional to the square of a characteristic length of the pore and, by implication, to the surface area. While the driving potential of the process may well reside predominantly in the surface free energy of the pores, but considering the highly variable and complicated geometry of the pores, the surface area is not necessarily correlated with an invariant value of two for the exponent, In any case, there is no reason to believe that in an essentially empirical power law formulation the mechanism of material transport would not also impact on the exponent value. Accordingly, we propose a generalized model of pore shrinkage with a floating exponent on the pore size:

$$\frac{\mathrm{d}r}{\mathrm{d}t} = -\frac{k}{r^{\mathrm{m}}} \tag{1}$$

where r is a characteristic pore dimension and k is a rate constant, with a temperature dependence that may be represented in the Arrhenius form as

$$k = k_0 e^{\left(\frac{-Q}{RT}\right)} \tag{2}$$

where k_0 is a constant, R the gas constant, Q is activation energy, and T the absolute temperature. It is understood that the effects of pore geometry and the mechanism of transport are embedded in the exponent m and, as such, it admits values other than 2 including non-integer values. Here we shall employ a formal population balance approach [25], a framework that is general enough to be applicable to pore shrinkage as well as grain growth in the intermediate and final stages of sintering. The continuity equation for the population balance on pores is given by:

$$\frac{\partial n(r,t)}{\partial t} + \frac{\partial}{\partial r}\left[n(r,t)\frac{\mathrm{d}r}{\mathrm{d}t}\right] = 0 \tag{3}$$

where $n(r, t)$ is the absolute frequency function such that $n(r, t)\mathrm{d}r$ is the number of pores in size range r to $r + \mathrm{d}r$ at sintering time t. The initial pore size distribution is given by:

$$n(r, 0) = n_0(r) \tag{4}$$

Moreover, the initial pore volume is:

$$V(0) = C\int_0^\infty n_0(r) r^3 \mathrm{d}r \tag{5}$$

where C is a dimensionless constant for given pore geometry. It is convenient to solve Eq. (3) by a transformation technique. Recognizing that in a well-behaved deterministic system the pores maintain their relative position in size, the following equality must hold for all times:

$$n(r, t)\mathrm{d}r = n_0(r_0)\mathrm{d}r_0 \tag{6}$$

where r_0 is related to r by the solution to Eq. (1):

$$r_0 = \left(r^{m+1} + (m+1)kt\right)^{1/(m+1)} \tag{7}$$

It also follows from Eq. (1) that:

$$\frac{\mathrm{d}r_0}{\mathrm{d}r} = \left(\frac{r}{r_0}\right)^m \tag{8}$$

Substituting Eqs. (7) and (8) into Eq. (6) yields:

$$n(r, t) = \frac{n_0([r^{m+1} + (m+1)kt]^{1/(m+1)})}{(1 + (m+1)ktr^{-(m+1)})^{1/(m+1)}} \tag{9}$$

The total pore volume is:

$$V(t) = C\int_0^\infty n(r, t) r^3 \mathrm{d}r \tag{10}$$

A cumulative pore volume distribution, $F_{\mathrm{V}}(r,t)$, defined as the normalized volume of pores larger than a size r is given by:

$$F_{\mathrm{V}}(r, t) = \frac{C}{V(0)}\int_r^\infty n(r', t) r'^3 \mathrm{d}r' \tag{11}$$

which will be used for comparing the model with experimental data.

3. Experimental procedure

Ceramic compacts were prepared from alumina (A16, Alcoa, USA) and Zirconia (SYP 5.2, Z.Tech, Australia) powders. Green samples were slipcast from slurries containing 30% solids by volume and deflocculated with dispersant Darvan C (Vanderbilt Co., USA). The casts were first dried and then sintered at 1400°C for 2, 6, 10 and 24 h. The electric furnace (Lindberg Model 51644) was heated at an average rate of 10°C/min to the peak temperature, held for the prescribed period and allowed to cool at its natural rate in a closed environment. The pore size distributions of the green and sintered samples were determined by mercury porosimetry (Micromeritics Model 9320[1]). The bulk densities of the compacts were measured by the Archimedes method using water as the immersion medium.

4. Results and discussion

4.1. Sintering of alumina and zirconia (our work)

We first present the results of the model and our experimental data on pore evolution during sintering of alumina and zirconia compacts. The initial pore size distribution data of the green compacts were first fitted to a lognormal volume-radius distribution and then transformed in a number-radius distribution:

---

[1] Courtesy Jawaharlal Nehru Aluminum Research Department and Design Centre, Nagpur.

$$n_0(r) = \frac{1}{r^4\sqrt{2\pi}\ln\sigma} e^{-\frac{1}{2}\left(\frac{\ln r - \ln r_m}{\ln\sigma}\right)^2} \quad (12)$$

where r_m, the geometric mean radius, and, the geometric standard deviation, were respectively, 0.034 and 1.2 for alumina samples (Fig. 1) and 4 and 1.4 for zirconia samples (Fig. 2). The higher porosity of the zirconia compacts is reflected in their pore size being much larger compared to those of the alumina compacts.

Fig. 1 compares the experimental and the simulated pore size distributions at various times for isothermal sintering of alumina at 1400°C. The numerical values of the model parameters, obtained by trial and error, are m = 3 and k = 4.9×10^{-8} μm^4/h. Similar comparison is presented in Fig. 2 for zirconia with model parameters m = 1 and k = 0.43 μm^2/h. The agreement, overall, is quite acceptable.

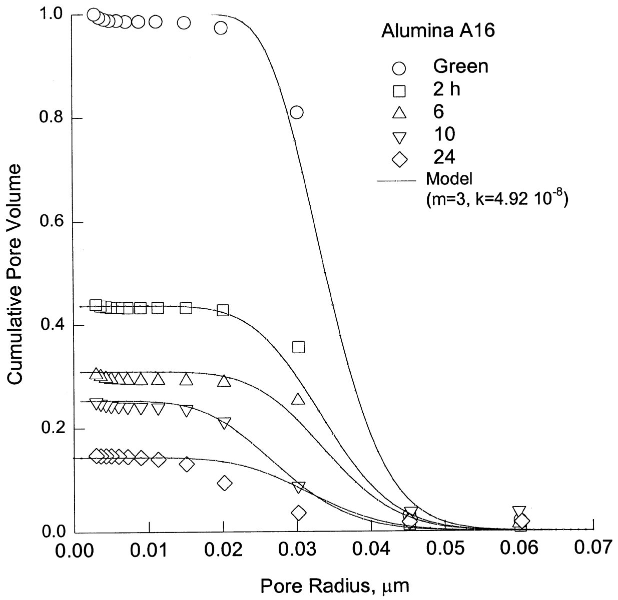

Fig. 1. Pore size distribution of alumina A16 compacts sintered at 1400°C: data and model.

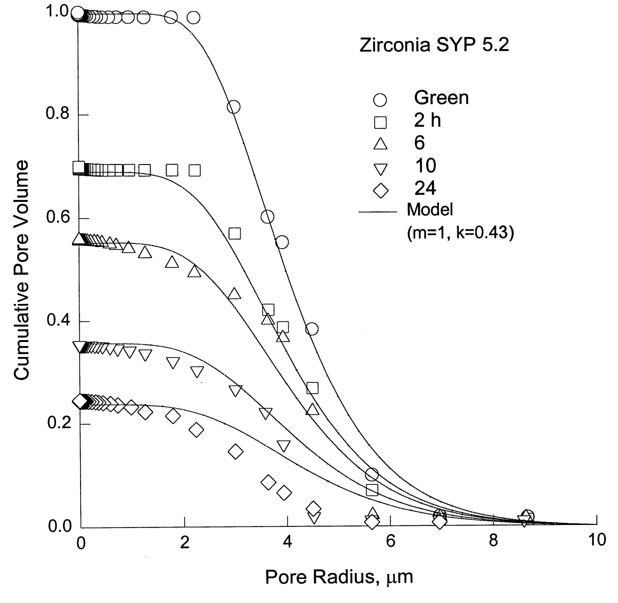

Fig. 2. Pore size distribution of zirconia SYP 5.2 compacts sintered at 1400°C: data and model.

4.2. Validation with other systems

For validating our model further, we have selected a few sintering systems from literature where data on pore evolution is reported. In this section we examine this published data on pore size evolution during sintering in the light of our model. Whittemore and Sipe [26] monitored the pore size distribution of a number of ceramic systems by mercury porosimetry. The green specimens were compacted by dry pressing and sintered for two hours at various temperatures. Fig. 3 shows one set of data for sintering of alumina compacts. Following Hogg and Hwang [21], the unfired data was represented by three size-segments and each segment was fitted to a lognormal distribution in the following manner:

$$\mathrm{LN}(r; r_m = 0.22, \quad \sigma = 0.145); \quad 0 < r \leqslant 0.0097\,\mu\mathrm{m}$$
$$\mathrm{LN}(r; r_m = 1.345, \quad \sigma = 2.93); \quad 0.0097 < r \leqslant 0.03\,\mu\mathrm{m}$$
$$\mathrm{LN}(r; r_m = 0.037, \quad \sigma = 1.30); \quad 0.03 < r\,\mu\mathrm{m}$$

As shown in Fig. 3, a good agreement between the data and the model could be obtained with the parameter $m = 4.5$. The activation energy Q is determined from a plot of log(k) vs $1/T$ shown as an inset. It was calculated to be 167 KJ/mol. Hogg and Hwang [21] reported 163 KJ/mol for this set of data. Fig. 4 includes another set of alumina data reported by Whittemore and Sipe [26]. In this case the parameters of the initial lognormal pore size distribution are $r_m = 0.02$ and $\sigma = 1.2$. The agreement between the model and the data is quite good, with the same value of 4.5 for the exponent m. The activation energy calculated from the plot shown in the inset is 207 KJ/mol.

Interestingly, the reported activation energies for densification of alumina by surface diffusion lie in the range of 230–280 KJ/mol [24]. On the other hand, based on a given value in his model of $m = 2$, Tomandl [22] calculated an activation energy of 376 KJ/mol for the densification of alumina which is unusually high, perhaps indicating that the value of m may be different from 2. Unfortunately his published data is not presented in a form that can be used for testing our model.

We now proceed to examine the published data on pore size evolution during sintering of cerium and yttrium oxides [27]. The powder compacts were prepared by cold isostatic pressing. Sintering was carried out at different temperatures for 3 h and pore size dis-

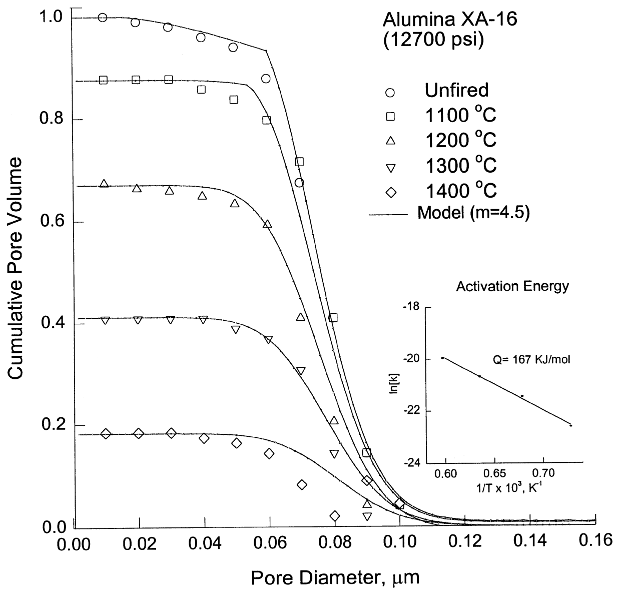

Fig. 3. Change in pore size distribution during sintering of alumina XA-16 compacted at 12700 psi [26] and model.

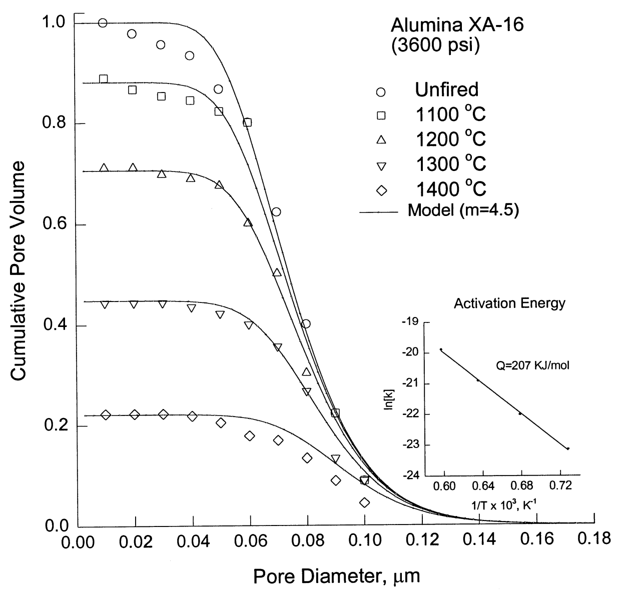

Fig. 4. Change in pore size distribution during sintering of alumina XA-16 compacted at 3600 psi [26] and model.

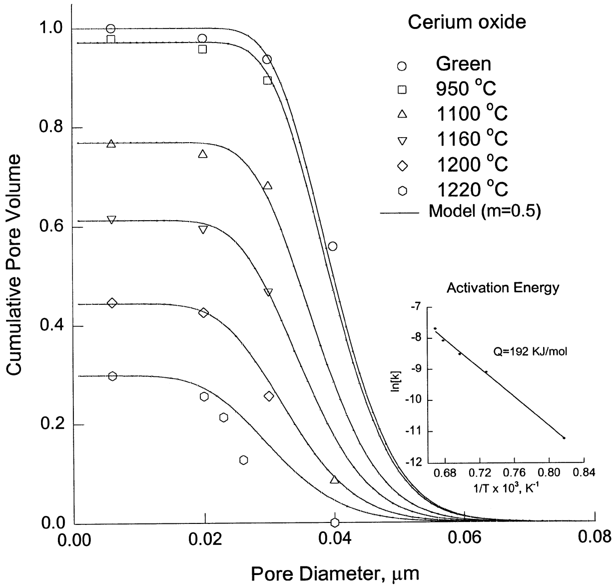

Fig. 5. Change in pore size distribution during sintering of cerium oxide [27] and model.

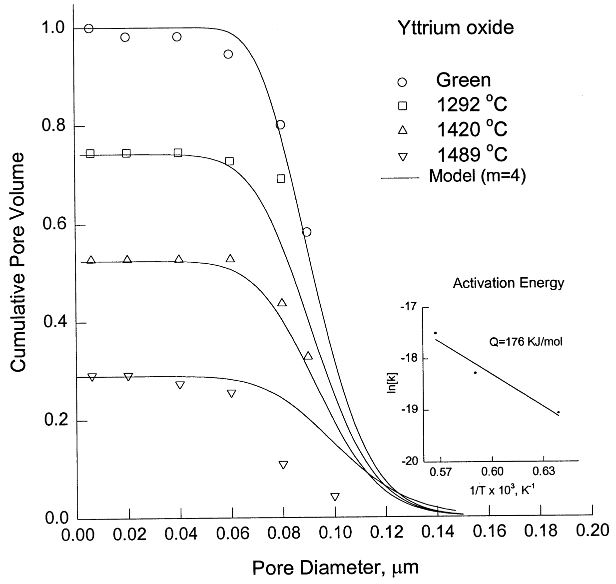

Fig. 6. Change in pore size distribution during sintering of yttrium oxide [27] and model.

tributions were measured using mercury porosimetry. Fig. 5 compares the pore size distribution data for CeO_2 along with the model generated curves. Here, $r_m = 0.02$ and $\sigma = 1.2$ for the pore size distribution of the green compact, and the shrinkage rate exponent $m = 0.5$. The activation energy was calculated to be 192 KJ/mol. Fig. 6 shows the data and the model for sintering of Y_2O_3 with $r_m = 0.047$, $\sigma = 1.24$ and $m = 4$. The corresponding activation energy is 176 KJ/mol.

5. Concluding remarks

A number of models in the literature for densification of sintered compacts often make use of the following empirical form for describing the rate of change of total pore volume [24, 28]:

$$\frac{dV}{dt} = f(V) \qquad (13)$$

In contrast to these lumped porosity models, the generalized treatment proposed here has the merit of providing the complete pore size distribution by virtue of the fact that it explicitly incorporates the pore shrinkage rate in a population balance model. One of the advantages of using the population balance approach is that the velocity or convective term can be generalized even beyond the simple power law provided, of course, adequate theoretical justification exists for such a choice. From the results presented here for sintering in realistic systems, it is seen that the model admits an exponent that is not necessarily equal to 2, as it has been proposed in the literature. It may range from less than one to greater than 4, depending upon the geometry of the pores and the mechanism of transport during sintering. We wish to reiterate that in our formulation we do not want to ascribe a particular mechanism of sintering corresponding to a value of m estimated using the data. It is a model parameter, which facilitates description of a practical sintering system in sufficient detail to be able to utilize it for optimization and control.

It is also reasonable to expect that the pore geometry, in turn, would depend on the powder size distribution, state of its aggregation and the consolidation method employed in forming the compact. In densification of aluminium, cerium and yttrium oxides at least, the estimated activation energies lie in the range of 167 to 207 KJ/mol, which are not unreasonable. The second part of the paper discusses in detail how the model developed here is embedded in a model for grain growth during solid-state sintering.

Acknowledgements

We gratefully acknowledge support for the work by US–India fund under the auspices of Department of Science and Technology (DST), India and National Institute of Standards and Technology (NIST), USA. Our sincere thanks to Professor E.C. Subbarao for his keen interest in this work.

References

[1] M. Randall, German, Sintering Theory and Practice, John Wiley & Sons, 1996, pp. 67–115.

[2] H.E. Exner, Principles of single phase sintering, Rev. Powder Met. Phys. Ceram. 1 (1979) 7–251.

[3] N.J. Shaw, Densification and coarsening during solid state sintering of ceramics: a review of the models, Powder Met. Int. 21 (3) (1989) 16–21.

[4] F.F. Lange, Sinterability of agglomerated powders, J. Am. Ceram. Soc. 67 (1984) 83–89.

[5] J. Zheng, J.S. Reed, Effects of particle packing characteristics on solid-state sintering, J. Am. Ceram. Soc. 72 (5) (1989) 810–817.

[6] J. Zhao, M.P. Harmer, Effect of pore distribution on microstructure development: III. Model experiments, J. Am. Ceram. Soc. 75 (4) (1992) 830–843.

[7] S.J. Penn, N.M. Alford, A. Templeton, X. Wang, M. Xu, M. Schrapel, K. Schrapel, Effect of porosity and grain size on the microwave dielectric properties of sintered alumina, J. Am. Ceram. Soc. 80 (7) (1997) 1885–1888.

[8] O. Flacher, J.J. Blandin, K.P. Plucknett, D.S. Wilkinson, C.H. Caceres, Effects of porosity on the superplastic properties of submicron alumina-zirconia composites, Mater. Sci. Forum 243–245 (1997) 411–416.

[9] A.L. Yurkov, T.A. Sarkisyan, D.A. Ivanov, R.C. Bradt, Final stages of sintering of ceramic materials: effect of residual porosity and microstructure on mechanical characteristics of surface, Ceram. Int. 23 (1997) 389–399.

[10] J.E. Burke, J.H. Rosolowski, Sintering, in: N.B. Hannay (Ed.), Reactivity of Solids, Treatise on Solid State Chemistry, Vol. 4, Plenum Press, New York, 1976, pp. 621–659.

[11] C. Wagner, Theorie der Alterung von Niederschagen durch Umlosen (Ostwald-Reifung), Z. Electro. Chem. 65 (1961) 581–591.

[12] I.M. Lifshitz, V.V. Slyozov, The kinetics of precipitation from super saturated solid solutions, J. Phys. Chem. Solids 19 (1961) 35–50.

[13] Pradip, Mathematical modelling and simulation of sintering systems, Trans., Powder Metallurgy Association of India 11 62–71 (1984).

[14] R.S. Gordon, D.D. Marchant, G.W. Hollenberg, Effect of small amounts of porosity on grain growth in hot-pressed magnesium oxide and magnesiowustite, J. Am. Ceram. Soc. 53 (7) (1970) 399–406.

[15] T. Sone, H. Akagi, H. Watarai, Effect of pore–grain boundary interactions on discontinuous grain growth, J. Am. Ceram. Soc. 74 (12) (1991) 3151–3153.

[16] T. Ikegami, M. Tsutsumi, S. Matsuda, S. Shirasaki, A model of densification with simultaneous grain growth, J. Appl. Phys. 49 (7) (1978) 4238–4241.

[17] J. Zhao, M.P. Harmer, Effect of pore distribution on microstructure development: II. First- and second-generation pores, J. Am. Ceram. Soc. 71 (7) (1988) 530–539.

[18] M.J. Mayo, D.C. Hague, Porosity-grain growth relationships in the sintering of nanocrystalline ceramics, Nanostruct. Mater. 3 (1–6) (1993) 43–52.

[19] J.H. Rosowlowski, C. Greskovich, Analysis of pore shrinkage by volume diffusion during final stage sintering, J. Appl. Phys. 44 (4) (1973) 1441–1450.

[20] H.E. Exner, G. Petzow, A critical evaluation of shrinkage equations, in: G.C. Kuczynski (Ed.), Sintering Processes, Materials Science Research, Plenum Press, New York, 1979, pp. 107–120.

[21] R. Hogg, C.L. Hwang, Pore size distributions in the sintering and heat treatment of agglomerated particulates, in: K.V.S. Sastry (Ed.), Agglomeration 77, A.I.M.E, New York, 1977, pp. 198–216.

[22] G. Tomandl, Computer calculations of sintering of polycrystalline ceramics, in: K.J. deVries (Ed.), Science of Ceramics, Vol. 9, The Netherlands Ceramic Society, Tiel, 1977, pp. 158–167.

[23] A.J. Markworth, J.K. McCoy, Computer simulation of effects of the pore size dstribution on the kinetics of pressure-assisted final-stage densification, J. Mater. Sci. 22 (1987) 488–494.

[24] M.N. Rahaman, Ceramic processing and sintering, Marcel Dekker, 1995, pp. 679–752.

[25] A.D. Randolph, M.A. Larson, Theory of Particulate Processes, Academic Press, 1971.

[26] O.J. Whittemore, J.J. Sipe, Pore gowth during the initial stages of sintering ceramics, Powder Technol. 9 (1974) 159–164.

[27] P.-L. Chen, I-W. Chen, Sintering of fine oxide powders: I. Microstructural evolution, J. Am. Ceram. Soc. 79 (12) (1996) 3129–3141.

[28] D.L. Johnson, A general model for the intermediate stage of sintering, J. Am. Ceram. Soc. 53 (10) (1970) 574–577.